The Astrophysical Journal, 782:46 (7pp), 2014 February 10 doi:10.1088/0004-637X/782/1/46

DEPOPULATION OF METASTABLE HELIUM BY RADIATIVE ASSOCIATION WITH HYDROGEN AND LITHIUM IONS

L. Augustovičová[1], W. P. Kraemer[2], and P. Soldán[1]
[1] Charles University in Prague, Faculty of Mathematics and Physics, Department of Chemical Physics and Optics, Ke Karlovu 3, CZ-12116 Prague 2, Czech Republic; pavel.soldan@mff.cuni.cz
[2] Max-Planck Institute of Astrophysics, Postfach 1371, D-85741 Garching, Germany
Received 2013 September 11; accepted 2013 December 19; published 2014 January 24

ABSTRACT

Depopulation of metastable He(2^3S) by radiative association with hydrogen and lithium ions is investigated using a fully quantal approach. Rate coefficients for spontaneous and stimulated radiative association of the HeH^+, HeD^+, and $LiHe^+$ molecular ions on the spin-triplet manifold are presented as functions of temperature considering the association to rotational-vibrational states of the lowest triplet electronic states $a^3\Sigma^+$ and $b^3\Sigma^+$ from the continuum states of the $b^3\Sigma^+$ electronic state. Evaluation of the rate coefficients is based on highly accurate quantum calculations, taking into account all possible state-to-state transitions at thermal energies (for spontaneous association) or at higher background energies (stimulated association). As expected, calculations show that the rate coefficients for radiative association to the *a* state are several orders of magnitude larger than the one for the *b* state formation. A noticeable effect by blackbody background radiation on the radiative association is only obtained for the $b \rightarrow b$ process. Aspects of the formation and abundance of the metastable $HeH^+(a^3\Sigma^+)$ in astrophysical environments are briefly discussed.

Key words: atomic data – atomic processes – molecular data – molecular processes

Online-only material: color figures

1. INTRODUCTION

Metastable helium 2^3S with its electronic configuration ($1s2s$) lying as much as 19.75 eV above the helium 1^1S_0 ground state has been found to have an unusually long lifetime of about two hours (Drake 1971; Hodgman et al. 2009). This extreme metastable life time arises from the fact that the direct photon decay to the ground state is doubly forbidden by quantum mechanical selection rules.

In view of the relatively large abundance of helium in the interstellar space, astrophysical consequences of the possible formation of its metastable levels were discussed early (Struve et al. 1939). It was then postulated that the excited (2^3S) state can be populated either by recombination from the ionized state or by collisional excitations from the neutral ground state by thermal electrons (Zeldovich et al. 1966). These processes can only produce a significant population of the metastable state if the gas temperature is high enough—such as, for instance, in planetary nebulae (Rees et al. 1968). Using a simple reaction network in which cosmic ray ionized helium recombines with electrons to form the metastable helium triplet and relying on the fact that spontaneous emission to the ground state level is forbidden, Scherb (1968) and Rees et al. (1968) suggested that interstellar metastable helium should be observable. However, whereas in these earlier studies two-photon emission from the metastable triplet was thought to be the dominant depopulation process (see also Robbins 1968), depopulations through excitations to higher excited helium levels are now considered to be most effective in energetic environments.

Especially due to its long lifetime, the He(2^3S) can act as an efficient base for the He I*λ10830 ($2s \rightarrow 2p$) and He I*λ3889 ($2s \rightarrow 3p$) absorption lines, which are suitable for measuring the He^+ fraction and column density in the outflows of active galaxies (Indriolo et al. 2009; Leighly et al. 2012). Observations of the λ10830 absorption line are reported for the Orion nebula (Boyce & Ford 1966) and BALQSO (Leighly et al. 2011), the λ3889 line toward ζ Ophiuchi (Galazutdinov & Krelowski 2012), and the λ3889 and λ3188 (due to $2s \rightarrow 4p$) lines from the Scorpii SN 2007 (Naito et al. 2013). Apart from these excitations to higher levels, depopulation of the 2^3S state in more dense plasmas can occur via collisions in the photoionized gas.

In this context, the depopulation of He(2^3S) by collisions with He^+ ions was investigated in previous studies: via radiative association (RA), these collisions can lead to the formation of helium ion dimer either in its electronic ground state ($X^2\Sigma_u^+$; Augustovičová et al. 2013a) or in the lowest excited quartet state ($b^4\Sigma_u^+$; Augustovičová et al. 2013b). In the present study, the corresponding RA processes of the He(2^3S) metastable with highly abundant protons as well as with Li^+ ions are investigated. The corresponding processes induced by dipole-moment continuum-bound transitions are described as

$$b^3[\mathrm{He}(2^3\mathrm{S}) + \mathrm{A}^+] \rightarrow \mathrm{HeA}^+(a^3\Sigma^+) + h\nu \quad (b \rightarrow a), \quad (1)$$

$$b^3[\mathrm{He}(2^3\mathrm{S}) + \mathrm{A}^+] \rightarrow \mathrm{HeA}^+(b^3\Sigma^+) + h\nu \quad (b \rightarrow b), \quad (2)$$

where $^3[\ldots]$ means a triplet submanifold of the corresponding collisional continuum and A is H, D, or Li. According to this scheme, reactions (1) and (2) start from collisions of helium in the metastable state 2^3S with hydrogen or lithium ions, and then proceed via resonance and continuum states of the $b^3\Sigma^+$ potential of the collisional complex to form (under spontaneous photon emission) the molecular ion in the triplet states $a^3\Sigma^+$ or $b^3\Sigma^+$. These processes are characterized as $b \rightarrow a$ and $b \rightarrow b$ in the following text. Apart from spontaneous emission, the corresponding processes stimulated by the background radiation (Stancil & Dalgarno 1997; Zygelman et al. 1998) are also considered.

2. METHODS

Our attempt to investigate RA is based on the approach of Zygelman & Dalgarno (1990) and Stancil & Dalgarno

(1997) and has been used in our previous work (Augustovičová et al. 2012, 2013a, 2013b). Including the possibility of dipole-moment transitions in the presence of the blackbody radiation field characterized by temperature T_b, the individual cross section for the transition between a continuum state with a positive energy E and orbital angular momentum J' to bound rovibrational states with vibrational quantum number v'' and orbital angular momentum J'' can be expressed as

$$\sigma_{J';v,''J''}(E;T_b) = \frac{1}{4\pi\epsilon_0}\frac{64}{3}\frac{\pi^5}{c^3\,k^2}\,p\,\nu^3_{E;v,''J''}\,S_{J',J''}\,M^2_{E,J';v,''J''} \times\left[\frac{1}{1-\exp\left(-h\nu_{E;v,''J''}/k_BT_b\right)}\right], \quad (3)$$

where c is the speed of light in a vacuum, $k^2 = 2\mu E/\hbar^2$, μ is the "charge-modified reduced mass" (Watson 1980) of the molecular ion ($\mu = 1467.778424$ a.u. for ^{4}HeH$^+$, $\mu = 2442.670838$ a.u. for ^{4}HeD$^+$, and $\mu = 4646.087837$ a.u. for ^{4}He^{7}Li$^+$), p is the probability of approach in the initial electronic state ($p = 1$ for both $b \to a$ and $b \to b$), and $\nu_{E;v,''J''}$ is the emitted photon frequency, $h\nu_{E;v,''J''} = E + \triangle E - E_{v,''J''}$, where $\triangle E_{b\to b} = 0$ eV, $\triangle E_{b\to a} = 8.8306602$ eV for HeH$^+$ and HeD$^+$, and $\triangle E_{b\to a} = 0.62394103$ eV for LiHe$^+$ (Kramida et al. 2011). $M_{E,J';v,''J''}$ is the matrix element of the transition dipole moment function between the initial continuum radial wave function and the final bound-state radial wave function. For dipole moment transitions of a heteronuclear diatomic molecule within the Hund's case (a) spinless approximation (Hansson & Watson 2005), the only non-zero Hönl-London coefficients are $S_{J',J'+1} = J' + 1$ and $S_{J',J'-1} = J'$.

The radial wave functions are determined by numerical integration of the corresponding Schrödinger equations using the Numerov–Cooley method (Numerov 1933; Cooley 1961). Resonance positions and tunneling widths were calculated employing the computer program LEVEL 7.7 (Le Roy 2005) and making use of the Airy-function boundary condition at the outermost classical turning point (Le Roy & Liu 1978) and the uniform semiclassical method (Connor & Smith 1981; Huang & Le Roy 2003).

For evaluation of the radial wave functions and the dipole-moment matrix elements, the potential energy and dipole-moment functions were represented numerically by a one-dimensional reciprocal-power reproducing kernel Hilbert space (RP-RKHS) interpolation method (Ho & Rabitz 1996), which allows for qualitatively correct extrapolation in the long-range region and it also allows for using predetermined values of long-range coefficients Ho & Rabitz (2000). In the case of potential energy curves, the interpolation was done with respect to r^2 (Soldán & Hutson 2000) using RP-RKHS parameters $m = 1$ and $n = 2$, and the coefficient D_4, which is equal to α_d(A)/2, was kept fixed to the values given by static dipole polarizabilities (α_d[He(2^3S)] = 315.631468 a.u., Yan & Babb 1998; α_d[H(1^2S)] = 4.5 a.u., Sewell 1949; and α_d[Li(2^2S)] = 162.87 a.u., Wansbeek et al. 2008).

Ab initio interaction energies for the $a^3\Sigma^+$ and $b^3\Sigma^+$ electronic states of HeH$^+$, and the corresponding dipole-moment values were calculated within the Born–Oppenheimer approximation. The aug-cc-pV6Z basis sets augmented by sets of (1s,2p,1d,1f) even-tempered diffuse functions were used for He and H; in order to increase the basis-set flexibility, a set of (4s, 4p) mid-bond functions was also added. A multi-reference configuration interaction (MRCI) method with single and double excitations (Werner & Knowles 1988; Knowles & Werner 1988), as implemented in MOLPRO (Werner & Knowles 2010), was employed with the active space formed by $14\sigma^+$ and 5π orbitals (the actual calculations were performed within the C_{2v} point-group symmetry using $14a_1$, $5b_1$, and $5b_2$ orbitals). The MRCI calculations were preceded by complete active space self-consistent field calculations (Werner & Knowles 1985; Knowles & Werner 1985) with the active space formed by $11\sigma^+$ and 3π orbitals ($11a_1$, $4b_1$, and $4b_2$ orbitals in the C_{2v} point-group symmetry). All interaction energies were calculated in the supermolecular manner and no counterpoise correction was applied to the MRCI interaction energies. The transition dipole-moment function was calculated with respect to the center of mass of the molecular ion (the position of the center of mass was determined using the standard atomic weights). The same Born–Oppenheimer potential energy curves and dipole moments were used for HeD$^+$. In the case of LiHe$^+$, the corresponding highly accurate potential energy curves and dipole moments obtained recently by Soldán & Kraemer (2012) were used.

The rate coefficient for formation of a molecule by (spontaneous and stimulated) RA at temperature T is defined by

$$k(T;T_b) = \left(\frac{8}{\mu\pi}\right)^{1/2}\left(\frac{1}{k_BT}\right)^{3/2}\int_0^\infty E\,\sigma(E;T_b)\,e^{-E/k_BT}\,dE, \quad (4)$$

where $\sigma(E;T_b)$ is the total cross section for RA, i.e., the sum of individual cross sections presented in Equation (3) over all allowed transitions. When evaluating this integral, we followed the approach of Augustovičová et al. (2012), where contributions from wide and narrow resonances are treated separately from the background contribution. It is often convenient to use some simple analytical form to represent the numerical values of the rate coefficients. In the present study, we use the Arrhenius-type function

$$f(T) = \alpha\left(\frac{T}{300}\right)^\beta e^{-\gamma/T}, \quad (5)$$

where α, β, and γ are the fitting parameters. In order to keep the maximum relative error below 10%, the temperature range is divided into several intervals.

3. RESULTS AND DISCUSSION

Potential energy curves for HeH$^+$ calculated in this work (shown together with the corresponding transition dipole moment in Figure 1) can be compared with the results obtained previously by others. For the $a^3\Sigma^+$ state, our equilibrium distance $R_e = 4.452\ a_0$ and dissociation energy relative to the potential minimum $\mathcal{D}_e = 851.9$ cm^{-1} compare very well with the results of Kolos (1976; $R_e = 4.455\ a_0$ and $\mathcal{D}_e = 850.0$ cm^{-1}) and those of Kraemer et al. (1995; $R_e = 4.452\ a_0$ and $\mathcal{D}_e = 840.6$ cm^{-1}), whereas the much smaller dissociation energy value obtained in the early calculations by Michels (1966; $\mathcal{D}_e = 656.5$ cm^{-1} at $R_e = 4.452\ a_0$) turns out to be close to the present $\mathcal{D}_0 = 666.9$ cm^{-1}, i.e., the dissociation energy relative to the ground vibrational level. For the $b^3\Sigma^+$ state, our equilibrium distance $R_e = 7.720\ a_0$ and dissociation energy $\mathcal{D}_e = 5848.1$ cm^{-1} are in reasonable agreement with the values obtained earlier by Michels (1966; $R_e = 7.754\ a_0$ and $\mathcal{D}_e = 5907.2$ cm^{-1}). The numbers of vibrational and rovibrational levels supported by these potentials are given in Table 1 for the two isotopologues HeH$^+$ and HeD$^+$ as well as for LiHe$^+$. For HeH$^+$ and HeD$^+$ they are in perfect agreement

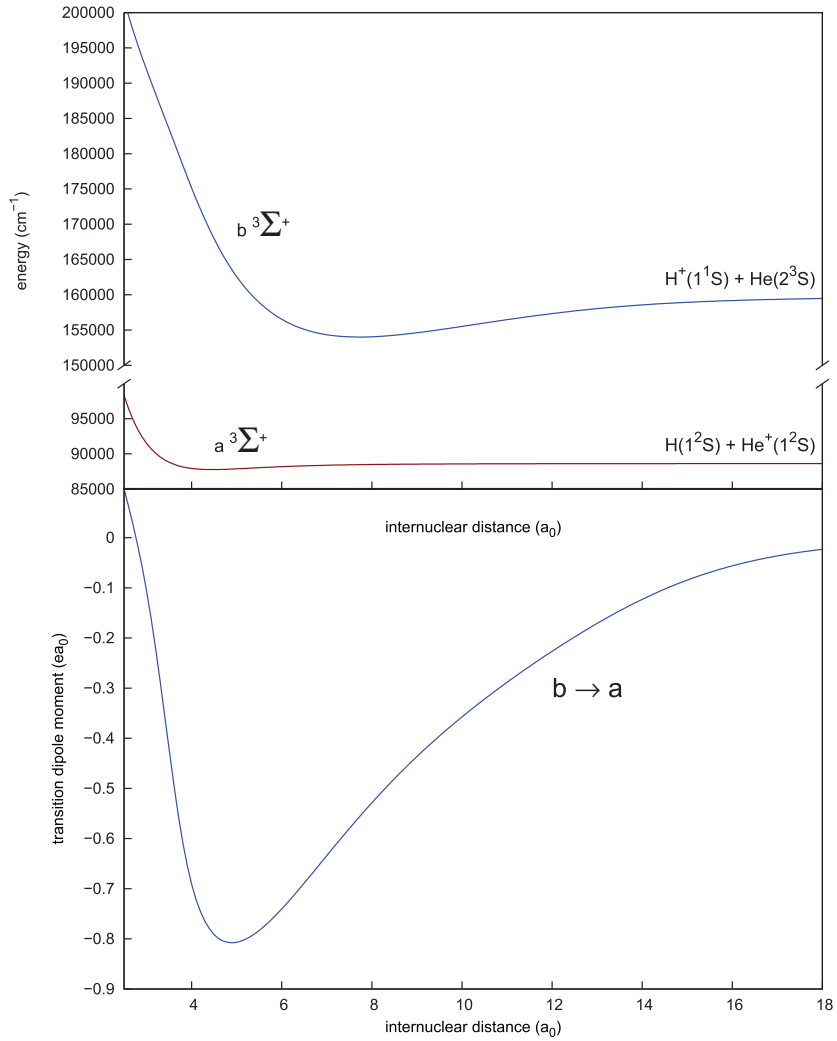

Figure 1. Potential energy curves and the transition dipole moment of HeH^+. The energy scale zero is set to the $H^+(1^1S)$ + $He(1^1S)$ dissociation limit. (A color version of this figure is available in the online journal.)

Table 1
Process Characteristics for Radiative Association of $He(2^3S)$ with Hydrogen and Lithium Ions

System	Process	n_{tot}	n_r	n_w	n_n	$\mathcal{D}_0$ (cm^{-1})	n_v	n_{rv}
HeH^+	$b \rightarrow a$	214	6	5	1	666.9	6	51
	$b \rightarrow b$	214	162	86	76	5652.4	35	1325
HeD^+	$b \rightarrow a$	353	7	7	0	706.4	8	85
	$b \rightarrow b$	353	266	122	144	5696.2	45	2209
$LiHe^{+a}$	$b \rightarrow a$	214	214	122	92	8181.1	61	4172
	$b \rightarrow b$	214	168	92	76	829.5	33	1289

Notes. Using the formalism of Augustovičová et al. (2012), n_{tot} is the total number of orbital resonances supported by the initial electronic states, from which n_r is the number of symmetry-allowed resonances, n_w is the number of wide resonances, and n_n is the number of narrow resonances; $\mathcal{D}_0$ is the dissociation energy of the target electronic state from the ground ($v'' = 0$, $J'' = 0$) rovibrational state, n_v is the number of bound vibrational ($J'' = 0$) states of the target electronic state, and n_{rv} is the total number of bound rovibrational states of the target electronic state.
[a] From Soldán & Kraemer (2012), the CCSD(T) potential energy curve is used for the $a^3\Sigma^+$ state and the MRCI potential energy curve is used for the $b^3\Sigma^+$ state.

with results of Yousif et al. (1994) and Chibisov et al. (1996). In the case of the $a^3\Sigma^+$ state, the last supported vibrational levels are $E_{v=5} = 1.082$ cm^{-1} and $E_{v=7} = 0.323$ cm^{-1} for HeH^+ and HeD^+, respectively. In the case of the much deeper $b^3\Sigma^+$ state potential, the highest bound vibrational levels are $E_{v=34} = 9.59 \times 10^{-4}$ cm^{-1} and $E_{v=44} = 1.142 \times 10^{-4}$ cm^{-1} for HeH^+ and HeD^+, respectively. Compared to HeH^+ and HeD^+, the situation is reversed for $LiHe^+$: the $a^3\Sigma^+$ electronic state is much stronger bound than the $b^3\Sigma^+$ electronic state (Soldán & Kraemer 2012).

Cross sections for spontaneous ($T_b = 0$ K) RA of the $b \rightarrow a$ and $b \rightarrow b$ processes in the three dimer systems

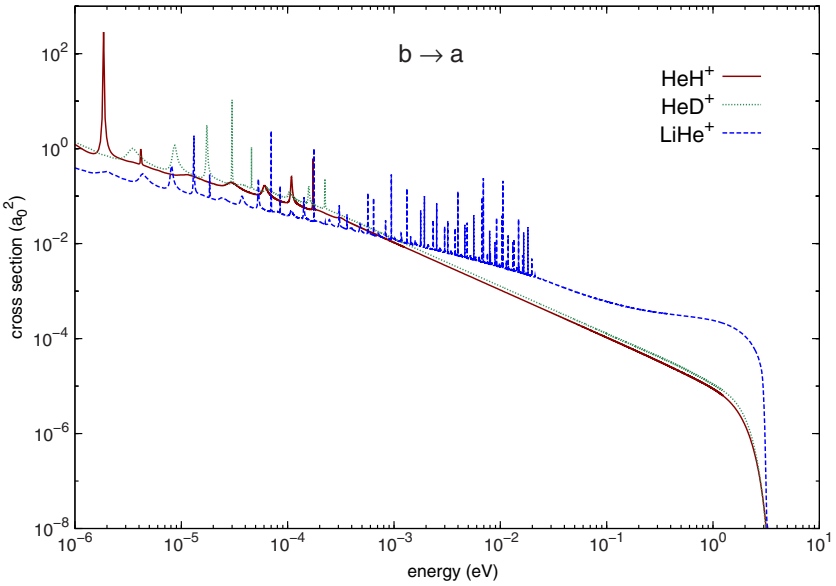

Figure 2. Cross sections for spontaneous ($T_b = 0$ K) radiative association process $b \rightarrow a$. Only the contribution of resonances wider than 0.01 cm^{-1} is shown. (A color version of this figure is available in the online journal.)

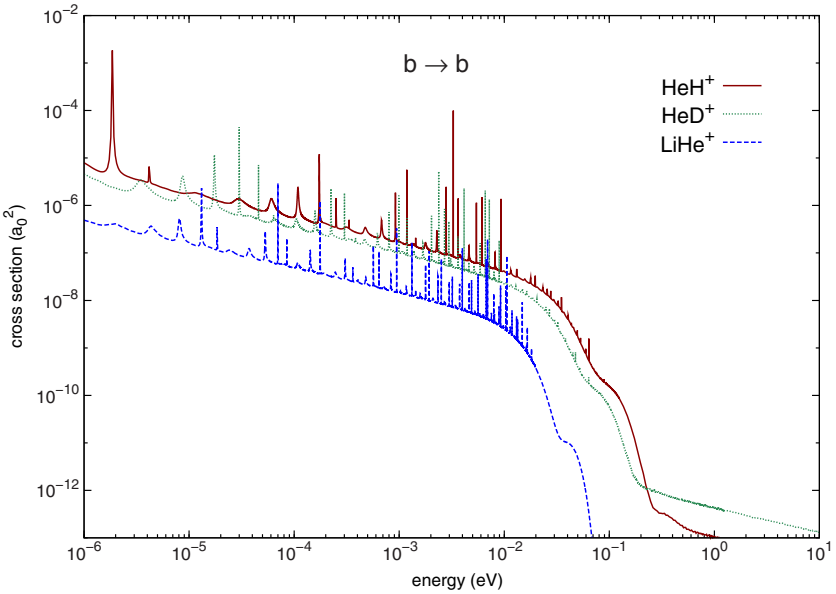

Figure 3. Cross sections for spontaneous ($T_b = 0$ K) radiative association process $b \rightarrow b$. Only the contribution of resonances wider than 0.01 cm^{-1} is shown. (A color version of this figure is available in the online journal.)

considered here (HeH^+, HeD^+, $LiHe^+$) are displayed in Figures 2 and 3, respectively. As expected the results obtained for the associations of He(2^3S) with H^+ or D^+ differ only marginally from each other. For the $b \rightarrow a$ processes, at least at lower energies, the cross section curves of the three association processes are very close to each other, whereas for $b \rightarrow b$ there is a substantial difference of about one order of magnitude between the cross section curve for the association with Li^+ compared to the others. The drop-off of the cross section curves for the $b \rightarrow a$ processes occurs at higher energies compared to $b \rightarrow b$.

The low-energy resonance structure of the RA cross sections, which is created by the quasi-bound states trapped behind the centrifugal barrier, is practically identical for the $b \rightarrow a$ and $b \rightarrow b$ processes in each of the three dimers. It seems that the fact that for each of the two processes the initial complex formation takes place on their respective b-state potentials is predominant for the cross section structure in this very low energy region. For the Li^+ association an obvious increase of the density of resonance lines in the medium energy region is observed. Especially for the $b \rightarrow a$ process, this should be due to the deep potential well of the $LiHe^+(a^3\Sigma^+)$ state potential with the larger number of bound rovibrational states in this target electronic state (see Table 1). For comparison, the number of the corresponding bound rovibrational states on the $HeH^+(a^3\Sigma^+)$ state potential curve is substantially smaller. On the other hand, as shown in Table 1, for the H^+ and D^+ associations the number of the bound rovibrational states in the $HeH^+(b^3\Sigma^+)$ target state potential is larger, leading to a denser resonance structure for the $b \rightarrow b$ processes in the medium energy region in Figure 3.

The corresponding rate coefficients for the spontaneous ($T_b = 0$ K) RA $b \rightarrow a$ process are plotted in Figure 4, and numerical

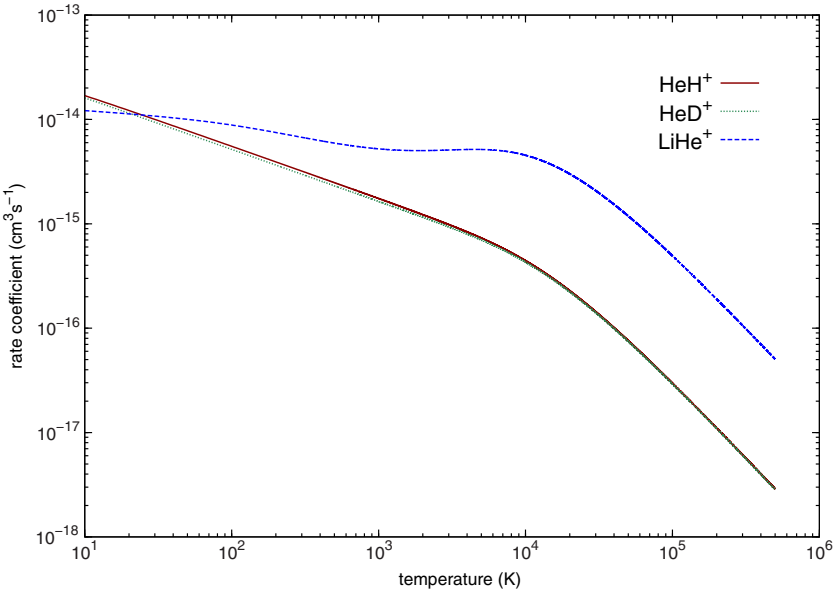

Figure 4. Rate coefficients for spontaneous ($T_b = 0$ K) radiative association $b \rightarrow a$ of He(2^3S) with hydrogen and lithium ions.
(A color version of this figure is available in the online journal.)

Table 2
Values of the Rate Coefficients (in cm^3 s^{-1}) for Radiative Association of He(2^3S) with Hydrogen and Lithium Ions[a]

T	HeH^+			HeD^+			$LiHe^+$		
(K)	$b \rightarrow a$[b]	$b \rightarrow b$[b]	$b \rightarrow b$[c]	$b \rightarrow a$[b]	$b \rightarrow b$[b]	$b \rightarrow b$[c]	$b \rightarrow a$[b]	$b \rightarrow b$[b]	$b \rightarrow b$[c]
10	1.69(−14)	3.71(−19)	1.94(−17)	1.61(−14)	1.64(−19)	1.03(−17)	1.22(−14)	1.45(−20)	1.36(−18)
20	1.22(−14)	3.54(−19)	1.67(−17)	1.15(−14)	1.43(−19)	8.28(−18)	1.13(−14)	1.30(−20)	1.13(−18)
30	1.00(−14)	3.30(−19)	1.47(−17)	9.39(−15)	1.31(−19)	7.19(−18)	1.08(−14)	1.19(−20)	9.83(−19)
50	7.79(−15)	2.87(−19)	1.19(−17)	7.29(−15)	1.14(−19)	5.81(−18)	1.00(−14)	9.93(−21)	7.65(−19)
100	5.53(−15)	2.18(−19)	8.10(−18)	5.16(−15)	8.56(−20)	3.90(−18)	8.84(−15)	6.60(−21)	4.63(−19)
200	3.92(−15)	1.43(−19)	4.76(−18)	3.65(−15)	5.41(−20)	2.21(−18)	7.50(−15)	3.54(−21)	2.32(−19)
500	2.48(−15)	6.21(−20)	1.85(−18)	2.31(−15)	2.22(−20)	8.14(−19)	5.94(−15)	1.21(−21)	7.49(−20)
1000	1.75(−15)	2.78(−20)	7.78(−19)	1.64(−15)	9.60(−21)	3.34(−19)	5.23(−15)	4.76(−22)	2.90(−20)
2000	1.22(−15)	1.13(−20)	3.03(−19)	1.16(−15)	3.82(−21)	1.28(−19)	5.03(−15)	1.78(−22)	1.07(−20)
2500	1.09(−15)	8.30(−21)	2.22(−19)	1.03(−15)	2.80(−21)	9.32(−20)	5.06(−15)	1.29(−22)	7.75(−21)
3000	9.85(−16)	6.44(−21)	1.71(−19)	9.36(−16)	2.17(−21)	7.17(−20)	5.10(−15)	9.88(−23)	5.93(−21)
4000	8.36(−16)	4.29(−21)	1.13(−19)	7.99(−16)	1.44(−21)	4.73(−20)	5.16(−15)	6.48(−23)	3.88(−21)
6000	6.49(−16)	2.40(−21)	6.26(−20)	6.24(−16)	8.09(−22)	2.61(−20)	5.10(−15)	3.56(−23)	2.13(−21)
8000	5.29(−16)	1.58(−21)	4.10(−20)	5.10(−16)	5.36(−22)	1.71(−20)	4.86(−15)	2.33(−23)	1.39(−21)
10000	4.43(−16)	1.14(−21)	2.95(−20)	4.29(−16)	3.90(−22)	1.23(−20)	4.54(−15)	1.67(−23)	9.97(−22)
16000	2.88(−16)	5.73(−22)	1.47(−20)	2.80(−16)	2.02(−22)	6.12(−21)	3.54(−15)	8.30(−24)	4.94(−22)
20000	2.28(−16)	4.13(−22)	1.06(−20)	2.23(−16)	1.49(−22)	4.40(−21)	3.00(−15)	5.95(−24)	3.54(−22)
25000	1.78(−16)	2.98(−22)	7.57(−21)	1.74(−16)	1.11(−22)	3.16(−21)	2.48(−15)	4.27(−24)	2.54(−22)
32000	1.33(−16)	2.07(−22)	5.24(−21)	1.30(−16)	8.09(−23)	2.19(−21)	1.95(−15)	2.95(−24)	1.75(−22)
50000	7.59(−17)	1.09(−22)	2.69(−21)	7.45(−17)	4.80(−23)	1.13(−21)	1.19(−15)	1.52(−24)	8.98(−23)
64000	5.47(−17)	7.63(−23)	1.86(−21)	5.38(−17)	3.69(−23)	7.84(−22)	8.79(−16)	1.05(−24)	6.21(−23)
100000	2.97(−17)	4.05(−23)	9.55(−22)	2.92(−17)	2.34(−23)	4.06(−22)	4.93(−16)	5.44(−25)	3.18(−23)
200000	1.11(−17)	1.53(−23)	3.39(−22)	1.09(−17)	1.12(−23)	1.47(−22)	1.90(−16)	1.95(−25)	1.13(−23)
500000	2.89(−18)	4.13(−24)	8.61(−23)	2.85(−18)	3.65(−24)	3.79(−23)	5.04(−17)	5.00(−26)	2.85(−24)

Notes.
[a] $x(-y) \equiv x \times 10^{-y}$.
[b] Spontaneous process ($T_b = 0$ K).
[c] Stimulated process ($T_b = 10{,}000$ K).

values for the $b \rightarrow a$ and $b \rightarrow b$ processes, evaluated at selected temperatures, are provided in Table 2. In Table 3, the values of the fitted parameters from the Arrhenius-type function (5) are presented for the dominant $b \rightarrow a$ process. As expected, the rate coefficients for the $b \rightarrow b$ RA processes are very small because of $\triangle E_{b \rightarrow b} = 0$. For the $b \rightarrow a$ processes the rates at very low temperatures between 10 and 100 K are rather similar for the three dimer systems considered here (in the range of 10^{-14} cm^3 s^{-1}). However, whereas the rate curves for HeH^+ and HeD^+ show the typical temperature fall off, the rate constant for the $LiHe^+$ association stays almost constant up to a temperature of about $T = 10{,}000$ K. The difference between the HeH^+ and the $LiHe^+$ curves at this temperature becomes about one order of magnitude (4.4×10^{-16} cm^3 s^{-1} versus 4.9×10^{-15} cm^3 s^{-1}).

Table 3
Values of the Arrhenius-function Parameters Representing the Rate Coefficients for the Spontaneous Radiative Association $b \rightarrow a$ of He(2^3S) with Hydrogen and Lithium Ions[a]

System	Process	T (K)	α ($cm^3\ s^{-1}$)	β	γ (K)
HeH^+	$b \rightarrow a$	1–1000	3.1998(−15)	−0.4994	0.2514
		1000–15000	8.7121(−15)	−0.8337	698.8793
		15000–500000	1.7782(−13)	−1.4829	8624.2387
HeD^+	$b \rightarrow a$	1–1000	2.9880(−15)	−0.4993	0.1525
		1000–15000	8.0080(−15)	−0.8190	698.3095
		15000–500000	1.7504(−13)	−1.4826	8818.9643
$LiHe^+$	$b \rightarrow a$	1–200	7.2229(−15)	−0.1733	0.2822
		200–5000	4.2584(−15)	0.0581	−136.5920
		5000–15000	1.7184(−13)	−0.8943	5014.2119
		15000–500000	3.0222(−12)	−1.4771	14201.5149

Note. [a] $x(-y) \equiv x \times 10^{-y}$.

This higher $LiHe^+$ association rate corresponds to the finding that the cross sections for the $b \rightarrow a$ process for $LiHe^+$ are larger at higher energies.

Our results for the spontaneous RA $b \rightarrow a$ of HeH^+ can be compared with the very recent theoretical study dedicated to the formation of HeH^+ in the metastable triplet state $a^3\Sigma^+$ (Loreau et al. 2013). At lower temperatures, our rate coefficients for this process are almost an order of magnitude larger than those of Loreau et al. (2013). Apart from using slightly different potential energy curves for the $a^3\Sigma^+$ and $b^3\Sigma^+$ states and different methods for the cross section calculations (the time-dependent wave packet method in the diabatic representation in Loreau et al. 2013 versus the time-independent method in the Born–Oppenheimer approximation in the present study), which leads overall to different cross sections in these two studies, the discrepancy is also caused by the inclusion of the low-energy RA cross sections into our rate-coefficient calculations. Furthermore, several shape resonances in this low-energy region (up to 10^{-3} eV, see Figure 2 and Table 1) contribute to the corresponding rate coefficient at lower temperatures as well.

Stimulated RA is relevant only for processes with very small $\triangle E$, where it can lead to an increase of the rate coefficients by up to two orders of magnitude (for moderate background temperatures up to $T_b = 10{,}000$ K). That is why in our study the stimulation of RA by background blackbody radiation concerns only the $b \rightarrow b$ process. The calculated increase at $T_b = 10{,}000$ K in the rate coefficients is indeed two orders of magnitude (see Table 2), similar to He_2^+ (Augustovičová et al. 2013a, 2013b). Even then, it results in the values of the corresponding rate coefficients of the order of (10^{-17} $cm^3\ s^{-1}$) at low temperatures. This is still much smaller than the rate coefficients of the spontaneous $b \rightarrow a$ process.

In previous studies, the depopulation of He(2^3S) via RA reactions with the He^+ ions was investigated leading to the formation of He_2^+ either in its electronic ground state ($X^2\Sigma_u^+$; Augustovičová et al. 2013a) or in the lowest excited quartet state ($b^4\Sigma_u^+$; Augustovičová et al. 2013b). Comparison of the rate coefficients obtained in these calculations with the present results shows that at very low temperatures between 10 and 100 K only the rate for the He_2^+ ground state formation has a magnitude comparable to the present rates, whereas the rate obtained for the quartet state formation is about two orders of magnitude smaller. At high temperatures, $T = 10{,}000$ K, magnitudes of the rates for the both helium-dimer ion formations are similar to the HeH^+ or HeD^+ association rates (in the range of 10^{-16} $cm^3\ s^{-1}$) with $LiHe^+$ association being about one order of magnitude higher.

4. CONCLUSION

RA processes between the very long-lived He(2^3S) metastable atom and the atomic ions H^+, D^+, and Li^+ producing the HeH^+, HeD^+, or $LiHe^+$ dimers in their $a^3\Sigma^+$ and $b^3\Sigma^+$ excited triplet states are investigated in this study. The dynamic calculations are based on highly accurate state-of-the-art ab initio calculations of the $a^3\Sigma^+$ and $b^3\Sigma^+$ state interaction potentials of HeH^+ and $LiHe^+$ and the associated transition dipole-moment functions. Characteristics of these states such as equilibrium bond distances R_e and $\mathcal{D}_e$ are in the case of HeH^+ in excellent agreement with the benchmark calculations of Kolos (1976). In the case of $LiHe^+$, the corresponding highly accurate potential energy curves and dipole moments obtained recently by Soldán & Kraemer (2012) are used.

Cross sections for the spontaneous ($T_b = 0$ K) RA for the $b \rightarrow a$ and $b \rightarrow b$ RA processes are calculated as functions of collision energy. The corresponding rate coefficients characterizing the efficiency of the formation of the dimer ions in their $a^3\Sigma^+$ and $b^3\Sigma^+$ triplet states are obtained as functions over a wide range of temperatures. Due to the large differences between the ionization energies of He and Li or He and H, the two-state $b \rightarrow a$ processes are as expected by far the most efficient ones compared to the one-state $b \rightarrow b$ processes. With exception for the $LiHe^+$ formation reaction, the rates for the two other formation reactions are steadily decreasing with increasing reaction temperatures. The rate for the $LiHe^+$ formation reaction, however, remains more or less constant up to a temperature of about $T = 10{,}000$ K. Compared to previously studied depopulation reactions of the metastable He(2^3S) atom by collisions with He^+ ions the processes considered in the present study are more efficient in the low temperature region, and in the case of $LiHe^+$ formation even over a wider temperature range.

Collisional reactions of He(2^3S) with ions provide significant cooling in nebulae with low heavy-element abundances (Clegg 1987). The $a^3\Sigma^+$ state of HeH^+ thus formed according to the processes described here is metastable with a lifetime of 150 s (Loreau et al. 2010) because the direct radiative transition to the singlet ground state is spin-forbidden. In low density plasmas, photodissociation processes are then the dominant depopulation reactions rather than collisional destructions (Loreau et al. 2013). Assuming equilibrium conditions between radiative associative formation and photodissociative destruction of the $HeH^+(a^3\Sigma^+)$ and using information about the abundance of metastable helium in nebulae as a function of the He^+ and electron densities (Clegg 1987), Loreau et al. (2013) derived a number density for the metastable HeH^+ triplet state $n = 3 \times 10^{-10}$ cm^{-3}, a value which should be about an order of magnitude larger using the association rates obtained in this study. Although much less abundant than the ground state singlet species, it has been argued that the RA process forming the triplet could nonetheless be of importance in primordial chemistry (Lepp et al. 2002).

In competition with the two-state $b \rightarrow a$ RA processes studied here, radiative charge transfer (RCT) reactions become an important alternative for the heteroatomic dimers. Using the notation of the association processes listed above, the relevant RCT reactions can be described as

$$b^3[\mathrm{He}(2^3\mathrm{S}) + \mathrm{A}^+] \rightarrow a^3[\mathrm{He}^+(^2\mathrm{S}) + \mathrm{A}(^2\mathrm{S})], \quad (6)$$

where A substitutes for H, D, or Li. In contrast to RA, in the RCT reaction, transitions under spontaneous photon emission take place from the initial resonance/continuum levels on the *b*-state potential to the resonance/continuum levels on the target *a*-state potential leading to immediate dissociation. For dimer systems the energy of the higher continuum levels is simply converted into kinetic energy of the dissociation partners. Previous accurate state-to-state calculations have shown that the rate constants for these RCT reactions can be orders of magnitude larger than the rates for the associated RA processes. Work is in progress to investigate differences in the efficiencies of the two reaction types.

L.A. and P.S. appreciate support from the Charles University in Prague. L.A. acknowledges funding from the Grant Agency of the Charles University in Prague (GAUK grant No. 550112).

REFERENCES

Augustovičová, L., Špirko, V., Kraemer, W. P., & Soldán, P. 2012, CPL, 531, 59
Augustovičová, L., Špirko, V., Kraemer, W. P., & Soldán, P. 2013a, A&A, 553, A42
Augustovičová, L., Špirko, V., Kraemer, W. P., & Soldán, P. 2013b, MNRAS, 435, 1541
Boyce, P. B., & W. K. Ford, J. 1966, PASP, 78, 163
Chibisov, M. I., Yousif, F. B., Van der Donk, P. J. T., & Mitchell, J. B. A. 1996, PhRvA, 54, 4997
Clegg, R. 1987, MNRAS, 229, 31
Connor, J. N. L., & Smith, A. D. 1981, MolPh, 43, 397
Cooley, J. W. 1961, MaCom, 15, 363
Drake, G. W. F. 1971, PhRvA, 3, 908
Galazutdinov, G. A., & Krelowski, J. 2012, MNRAS, 422, 3457
Hansson, A., & Watson, J. K. G. 2005, JMoSp, 233, 169
Ho, T. S., & Rabitz, H. 1996, JChPh, 104, 2584
Ho, T. S., & Rabitz, H. 2000, JChPh, 113, 3960
Hodgman, S. S., Dall, R. G., Byron, L. J., et al. 2009, PhRvL, 103, 053002
Huang, Y., & Le Roy, R. J. 2003, JChPh, 119, 7398
Indriolo, N., Hobbs, L., Hinkle, K. H., & McCall, B. J. 2009, ApJ, 703, 2131
Knowles, P. J., & Werner, H.-J. 1985, CPL, 115, 259
Knowles, P. J., & Werner, H.-J. 1988, CPL, 145, 514
Kolos, W. 1976, IJQC, 10, 217
Kraemer, W. P., Špirko, V., & Juřek, M. 1995, CPL, 236, 177
Kramida, A., Ralchenko, Y., Reader, J., et al. 2011, NIST Atomic Spectra Database (version 5.0), See http://physics.nist.gov/asd3
Le Roy, R. J. 2005, LEVEL 7.7: A Computer Program for Solving the Radial Schrödinger Equation CPRR-661 (Ontario: University of Waterloo)
Le Roy, R. J., & Liu, W. K. 1978, JChPh, 69, 3622
Leighly, K. M., Dietrich, M., & Barber, S. 2011, ApJ, 728, 94
Leighly, K. M., Lucy, A. B., Dietrich, M., Terndrup, D., & Gallagher, S. C. 2012, in ASP Conf. Ser. 460, AGN Winds in Charleston, ed. G. Chartas, F. Hamann, & K. M. Leighly (San Francisco, CA: ASP), 72
Lepp, S., Stancil, P. C., & Dalgarno, A. 2002, JPhB, 35, R57
Loreau, J., Liévin, J., & Vaeck, N. 2010, JChPh, 133, 114302
Loreau, J., Vranckx, S., Desouter-Lecomte, M., Vaeck, N., & Dalgarno, A. 2013, JPCA, 117, 9486
Michels, H. H. 1966, JChPh, 44, 3834
Naito, H., Tajitsu, A., Arai, A., & Sadakane, K. 2013, PASJ, 65, 37
Numerov, B. 1933, MaCom, 2, 188
Rees, M. J., Sciama, D. W., & Stobbs, S. 1968, ApL, 2, 243
Robbins, R. R. 1968, ApJL, 151, L35
Scherb, F. 1968, ApJL, 153, L55
Sewell, G. L. 1949, PCPS, 45, 678
Soldán, P., & Hutson, J. M. 2000, JChPh, 112, 4415
Soldán, P., & Kraemer, W. P. 2012, CP, 393, 135
Stancil, P. C., & Dalgarno, A. 1997, ApJ, 479, 543
Struve, O., Wurm, K., & Henyey, L. 1939, PNAS, 25, 67
Wansbeek, L. W., Sahoo, B. K., Timmermans, R. G. E., Das, B. P., & Mukherjee, D. 2008, PhRvA, 78, 012515
Watson, J. K. G. 1980, JMoSp, 80, 411
Werner, H.-J., & Knowles, P. J. 1985, JChPh, 82, 5053
Werner, H.-J., & Knowles, P. J. 1988, JChPh, 89, 5803
Werner, H.-J., & Knowles, P. J. 2010, MOLPRO, version 2010.2: A Package of Ab Initio Quantum-chemistry Programs, See http://www.molpro.net
Yan, Z.-C., & Babb, J. F. 1998, PhRvA, 58, 1247
Yousif, F. B., Mitchell, J. B. A., Rogelstad, M., et al. 1994, PhRvA, 49, 4610
Zeldovich, Y. B., Novikov, I. D., & Sunyaev, R. A. 1966, Astron. Circ. U.S.S.R., No. 371
Zygelman, B., & Dalgarno, A. 1990, ApJ, 365, 239
Zygelman, B., Stancil, P. C., & Dalgarno, A. 1998, ApJ, 508, 151